

Synthesis of Thermosetting Polyetherimide-Containing Allyl Groups

Ching Hsuan Lin,^{1,2} Sheng Lung Chang,¹ Yu Ru Wang,¹ Chin Kuang Hsu,¹ Tzong Yuan Juang³

¹Department of Chemical Engineering, National Chung Hsing University, Taichung, Taiwan

²Center of Nanoscience & Nanotechnology, National Chung Hsing University, Taichung, Taiwan

³Department of Applied Chemistry, National Chiayi University, Chiayi, Taiwan

Correspondence to: C. H. Lin (E-mail: lynch@nchu.edu.tw) or T. Y. Juang (E-mail: tyjuang@mail.ncyu.edu.tw)

Received 14 October 2012; accepted 19 December 2012; published online 28 January 2013

DOI: 10.1002/pola.26549

ABSTRACT: An allyl-containing diphenol, 1-(3-allyl-4-hydroxyphenyl)-1-(4-hydroxyphenyl)-1-(6-oxido-6H-dibenz[c,e][1,2]oxaphosphorin-6-yl)ethane (**1**), was prepared from a one-pot reaction of 9,10-dihydro-oxa-10-phosphaphenanthrene-10-oxide, 4-hydroxyacetophenone, and 2-allylphenol in the presence of *p*-toluenesulfonic acid monohydrate. Then, an allyl-containing dietheramine, 1-(4-(4-aminophenoxy)phenyl)-1-(3-allyl-4-(4-aminophenoxy)-phenyl)-1-(6-oxido-6H-dibenz[c,e][1,2]oxaphosphorin-6-yl)ethane (**3**), was prepared from the nucleophilic substitution of (**1**) with 4-fluoronitrobenzene, followed by the reduction of the dinitro groups by Fe/HCl. A flexible polyetheri-

imide (PEI) (**4**) with a curable characteristic was prepared from the condensation of (**3**) and 4,4'-oxydiphthalic anhydride (ODPA) in *m*-cresol in the presence of isoquinoline. Curing PEI (**4**) at 300 °C leads to PEI (**5**), which exhibits much a higher T_g value (307 °C) and a lower coefficient of thermal expansion (CTE) (29 ppm/°C) than PEI (**4**) ($T_g = 253$ °C, CTE 52 ppm/°C). © 2013 Wiley Periodicals, Inc. *J. Polym. Sci., Part A: Polym. Chem.* **2013**, *51*, 1734–1741

KEYWORDS: allyl; high performance polymers; polyetherimide; polyimides; thermosets

INTRODUCTION Aromatic polyimides are widely applied in electronics and composites owing to their characteristics of high glass transition temperature, high thermal stability, and good mechanical properties.^{1–9} However, the good thermal properties are usually accompanied by poor solubility in organic solvents, limiting their processability. Various approaches have been developed to enhance their organosolubility including (1) the incorporation of thermally stable but flexible linkages, such as ether, methylene, sulfonyl, and hexafluoroisopropylidene^{10–12}; (2) introducing unsymmetrical linkages^{13–19} or bulky pendants;^{15,20–23} and (3) copolymerization.^{24–29}

Although organosoluble polyimides exhibit processability, they usually display decreased thermal properties compared with insoluble polyimides. Many thermosetting polyimides have been reported in the literature, most of them are terminated with crosslinkable linkages, such as phenylmaleic,³⁰ phenylethynyl,^{31,32} maleic,³³ nadic,^{34,35} allylic,³⁶ benzocyclobutene,³⁷ and carboxylic acid.³⁸ Thermosetting polyimide with crosslinkable linkage in the repeat unit is rarely reported.³⁹ Ueda and coworkers⁴⁰ prepared thermo-curable polyphenylene ether through the oxidative coupling copolymerization of 2-allyl-6-methylphenol with 2,6-dimethylphenol. The thermally cured copolymer showed excellent solvent resistance, high thermal stability, high T_g , a low dielectric constant, and a low dissipation factor. The above method

inspired us to synthesize an allyl-containing polyimide that can match the requirement of processability (before thermal curing) and good thermal properties (after thermal curing). Therefore, an organosoluble polyetherimide (PEI) (**4**) was prepared through the solution polymerization of an allyl-containing diamine (**3**) and 4,4'-oxydiphthalic anhydride (ODPA). Curing PEI (**4**) at 300 °C led to thermosetting PEI (**5**). The experimental data showed that (**5**) exhibited much higher T_g value and lower thermal expansion than (**4**). Detailed synthetic strategy and analysis are discussed in this study.

EXPERIMENTAL

Materials

9,10-Dihydro-9-oxa-10-phosphaphenanthrene 10-oxide (DOPO, from TCI), *p*-toluenesulfonic acid monohydrate (*p*-TSA, from Showa), 4-hydroxyacetophenone (from Acros), 2-allylphenol (from Showa), potassium carbonate (from Showa), 10% palladium on carbon (Pd/C, from Acros), 4-fluoronitrobenzene (from Acros), iron powder (Fe, from J. T. Baker), 37% hydrochloric acid (HCl, from Scharlau), and calcium hydride (from Acros) were used as received. ODPA (Chriskev) was recrystallized from acetic anhydride. *N,N*-dimethylacetamide (DMAc, from TEDIA) was purified by distillation under reduced pressure over calcium hydride (Acros) and stored over molecular sieves. The other solvents used are

Additional Supporting Information may be found in the online version of this article.

© 2013 Wiley Periodicals, Inc.

commercial products (HPLC grade), which were used without further purification.

Characterization

NMR measurements were performed using a Varian Inova 600 NMR in dimethyl sulfoxide (DMSO)- d_6 , and the chemical shift was calibrated by setting the chemical shift of DMSO- d_6 as 2.49 ppm. Differential scanning calorimeter (DSC) scans were obtained by a Perkin-Elmer DSC 7 in a nitrogen atmosphere at a heating rate of 20 °C/min. Dynamic mechanical analysis (DMA) was performed by a Perkin-Elmer Pyris Diamond DMA at a heating rate of 5 °C/min. Thermomechanical analysis (TMA) was performed by a SII TMA/SS6100 at a heating rate of 5 °C/min. Thermal gravimetric analysis (TGA) was performed with a Perkin-Elmer Pyris1 at a heating rate of 20 °C/min in nitrogen and air atmosphere, respectively. Elemental analysis (C, H, and N) was performed on an Elemental Vario EL III. The infrared spectra were recorded using a Nicolet Avatar 320 FTIR spectrophotometer and 32 scans were collected with a spectral resolution of 1 cm^{-1} . The flame retardancy of the PEIs was determined by a UL-94VTM vertical thin test. In that test, an 8" \times 2" sample was wrapped around a 1/2" mandrel, and then taped on one end. The mandrel was removed, leaving a cone-shaped sample that was relatively rigid. The two flame applications took 3 s each for the UL-94 VTM vertical thin film. After the first ignition, the flame was removed and the time for the polymer to self-extinguish (t_1) was recorded. Cotton ignition was noted if polymer dripping occurred during the test. After cooling, the second ignition was performed on the same sample and the self-extinguishing time (t_2) and dripping characteristics were recorded. If $t_1 + t_2 < 10$ s without any dripping, then the polymer was considered to be a VTM-0 material. If $t_1 + t_2$ was in the range of 10–30 s without any dripping, then the polymer was considered to be a VTM-1 material.

Synthesis of (1)

In brief, 10.81 g of DOPO (0.05 mol), 6.81 g of 4-hydroxyacetophenone (0.05 mol), 0.432 g of p-TSA (4 wt % based on the weight of DOPO), and 6.71 g of 2-allylphenol (0.15 mol) were introduced into a 100-mL round-bottomed glass flask equipped with a nitrogen inlet and a magnetic stirrer. The mixture was stirred at 60 °C for 12 h. After that, the reaction mixture was cooled to room temperature. The precipitate was filtered, washed with ethyl acetate, recrystallized by methanol, and dried at 100 °C in a vacuum oven. White crystal (yield, 70%) was obtained. Melting point (DSC) was 227 °C.

ELEM. ANAL. for $\text{C}_{29}\text{H}_{25}\text{O}_4\text{P}$: Calcd. C 74.35%, H 5.38%; Found C 74.25%, H 5.57%. $^1\text{H-NMR}$ (DMSO- d_6), $\delta = 1.58$ (3H, H^{14}), 3.09 (2H, H^{20}), 4.91 (2H, H^{22}), 5.78 (1H, H^{21}), 6.57 (3H, $\text{H}^{17,25}$), 6.96 (1H, H^{16}), 7.07–7.12 (4H, $\text{H}^{10,23,24}$), 7.14–7.20 (2H, $\text{H}^{4,8}$), 7.32–7.36 (2H, $\text{H}^{3,9}$), 7.66 (1H, H^2), 7.95 (1H, H^7), 8.07 (1H, H^1), 9.33–9.41 (2H, OH).

Synthesis of (2)

Briefly, 4.68 g of (1) (0.01 mol), 3.10 g of 4-fluoronitrobenzene (0.022 mol), 3.04 g of potassium carbonate (0.022

mol), and 30 mL of DMAc were introduced to a round-bottomed 100-mL glass flask equipped with a nitrogen inlet, a condenser, and a magnetic stirrer. The reaction mixture was heated to 110 °C and maintained at that temperature for 12 h. Then, the reaction mixture was filtered, and the filtrate was poured into 450 mL of methanol/water (1/5, v/v) solution under stirring. The precipitate was filtered and recrystallized from acetic anhydride, and then dried in a vacuum oven at 110 °C. Light yellow crystals (yield, 80%) were obtained. Melting point (DSC) was 184 °C.

ELEM. ANAL. for $\text{C}_{41}\text{H}_{31}\text{N}_2\text{O}_8\text{P}$: Calcd. C 69.29%, H 4.40%, N 3.94%; Found C 69.09%, H 4.52%, N 3.89%. $^1\text{H-NMR}$ (ppm, DMSO- d_6), $\delta = 1.85$ –1.90 (3H, H^{14}), 3.02–3.12 (2H, H^{20}), 4.83–4.95 (2H, H^{22}), 5.65 (1H, H^{21}), 6.88 (1H, H^{17}), 6.95 (2H, H^{28}), 7.08 (4H, $\text{H}^{25,28}$), 7.15 (1H, H^{10}), 7.21 (2H, $\text{H}^{8,16}$), 7.32 (1H, H^{23}), 7.38 (1H, H^9), 7.47 (3H, $\text{H}^{4,24}$), 7.52 (1H, H^3), 7.76 (1H, H^2), 8.07 (1H, H^7), 8.18 (1H, H^1), 8.26–8.30 (4H, $\text{H}^{29,29}$).

Synthesis of (3)

A mixture of 1.5 mL of 37% HCl and 3 mL of 50% aqueous ethanol was slowly added to a mixture of 5.0 g of (2) (7 mmol), 1.96 g of iron powder (35 mmol), and 15 mL of 50% aqueous ethanol in a three-necked, 100-mL, round-bottomed flask equipped with a nitrogen inlet and a magnetic stirrer. The mixture was stirred under reflux for 3 h, and then 1.3 mL of ammonium hydroxide solution (10 wt %) was slowly added to this mixture over a 1-h period. The mixture was hot-filtered, and the filtrate was poured into water. The precipitate was filtered and dried in a vacuum oven to afford diamine (3). Light orange crystals (yield, 70%) were obtained. Melting point (DSC) was 103 °C.

ELEM. ANAL. for $\text{C}_{41}\text{H}_{35}\text{N}_2\text{O}_4\text{P}$: Calcd. C 75.68%, H 5.42%, N 4.31%; found C 75.44%, H 5.57%, N 4.28%. $^1\text{H-NMR}$ (ppm, DMSO- d_6), $\delta = 1.70$ (3H, H^{14}), 4.23 (2H, H^{20}), 4.99 (6H, $\text{H}^{20}, \text{NH}_2$), 5.82 (1H, H^{21}), 6.37 (1H, H^{17}), 6.57 (4H, $\text{H}^{29,29}$), 6.65 (4H, $\text{H}^{25,28}$), 6.73 (2H, H^{28}), 6.97 (1H, H^{16}), 7.08 (1H, H^{10}), 7.20 (4H, $\text{H}^{8,23,24}$), 7.33 (1H, H^9), 7.37 (1H, H^4), 7.43 (1H, H^3), 7.70 (1H, H^2), 7.95 (1H, H^7), 8.07 (1H, H^1).

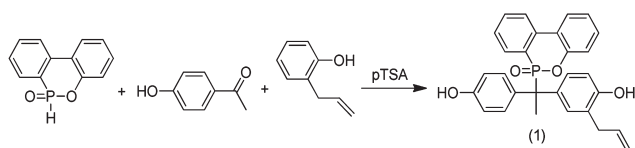
Preparation of (4) and (5)

PEI (4) was prepared by reacting (3) with an equal mole of ODP. To a 100-mL three-neck round-bottomed flask equipped with a magnetic stirrer, nitrogen inlet, 1.301 g of (3) (2 mmol), 0.436 g of ODP (2 mmol), 8.7 g of *m*-cresol, and two drops of isoquinoline were added. The mixture was reacted at 200 °C for 8 h. Then, the viscous solution was poured into methanol. The precipitate was filtered, dried, and dissolved in DMAc to afford a 20 wt % solution. The solution was casted on glass by an automatic film applicator, and dried at 60 °C (12 h), 100 °C (1 h), 150 °C (1 h), and 200 °C (1 h). Thermosetting PEI (5) was obtained by the thermal curing of (4) at 300 °C (1 h).

RESULTS AND DISCUSSION

Synthesis of (1)

The allyl-containing diphenol (1) was prepared in a one-pot procedure by the reaction of DOPO, 4-hydroxyacetophenone in excess 2-allylphenol using p-TSA as catalyst (Scheme 1).



SCHEME 1 Synthesis of (1).

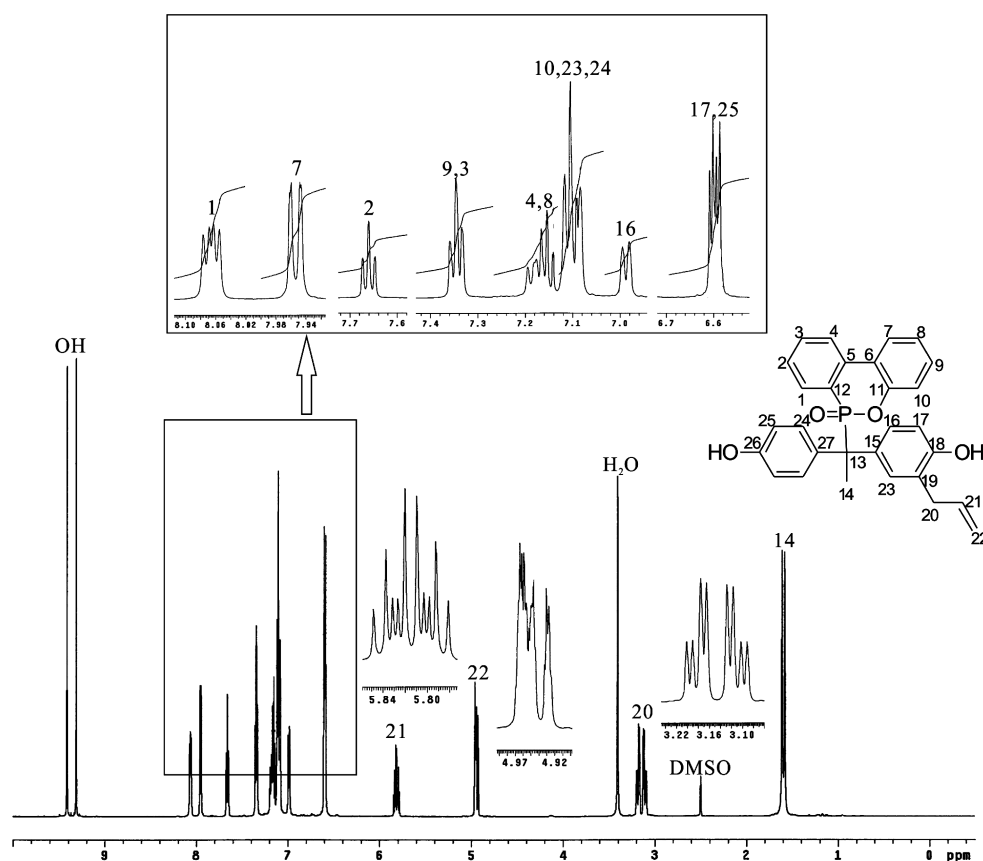
Supporting Information Scheme S1 shows the proposed mechanism for the synthesis of (1). In the mechanism, DOPO attacks the carbonyl group via a nucleophilic addition, forming a tertiary hydroxyl group. The tertiary hydroxyl group is then protonated by acid. Then, spontaneous dissociation of the protonated hydroxyl group occurs to yield a carbocation intermediate plus water. The carbocation can be stabilized by the electron-donating phenolic OH. Finally, 2-allylphenol reacts with the carbocation via an electrophilic substitution, yielding (1). Figure 1 shows the $^1\text{H-NMR}$ spectrum of (1). The signals of the methyl group (H^{14}) were split into two peaks with a coupling constant of 17.4 Hz owing to a $^3\text{J}_{\text{P-H}}$ coupling. Two phenol peaks at around 9.4 ppm, and the allyl signals at 5.8 (H^{21}), 4.9 (H^{22}), and 3.1 (H^{20}) were clearly observed. The peak patterns of Ar-H, assigned by the assistance of correlations shown in the $^1\text{H-}^1\text{H}$ COSY spectra (Supporting Information Fig. S1) confirmed the structure of (1). In the $^{13}\text{C-NMR}$ spectrum (Supporting Information Fig. S2), owing to the $^1\text{J}_{\text{P-C}}$ coupling, the signals of C^{13} split

into two peaks at 51.4 and 52.0 ppm with a coupling constant of 90 Hz. For the same reason, the signals of C^{12} split into two peaks at 122.3 and 123.1 ppm with a coupling constant of 110 Hz. The allyl signals at 136.9 (C^{21}), 115.4 (C^{22}), and 33.8 (C^{20}) were clearly observed. The peak patterns of Ar-C, assigned by the assistance of the correlations shown in the $^1\text{H-}^{13}\text{C}$ HETCOR spectra (Supporting Information Fig. S3) also confirmed the structure of (1).

The structure of (1) was further confirmed by the single crystal diffractogram (Fig. 2 and Supporting Information Table S1). The crystal of (1) belongs to the triclinic system with $a = 8.7431 \text{ \AA}$, $\alpha = 94.015^\circ$; $b = 14.4670 \text{ \AA}$, $\beta = 102.431^\circ$, and $c = 19.8130 \text{ \AA}$, $\gamma = 98.761^\circ$. The bond length for $\text{C}(21)\text{-C}(22)$ is 1.272 \AA , which is shorter than those of $\text{C}(20)\text{-C}(21)$ (1.535 \AA) and $\text{C}(13)\text{-C}(14)$ 1.455 \AA . The shorter bond length supports the finding that the $\text{C}(21)\text{-C}(22)$ is a double bond, and no isomerization of the allyl chains to propenyl moieties was found in the synthesis (to be discussed later).

Synthesis of (2)

Dinitro compound (2) was synthesized from the nucleophilic substitution of (1) and 4-fluoronitrobenzene at 110 $^\circ\text{C}$ using potassium carbonate as catalyst. Hamerton and coworkers⁴¹ reported the isomerization of allyl chains to propenyl moieties in the reaction of 2-allylphenol and *bis*(4-fluorophenyl)-sulfone in the presence of potassium carbonate. Therefore,

FIGURE 1 $^1\text{H-NMR}$ spectrum of (1) in $\text{DMSO-}d_6$.

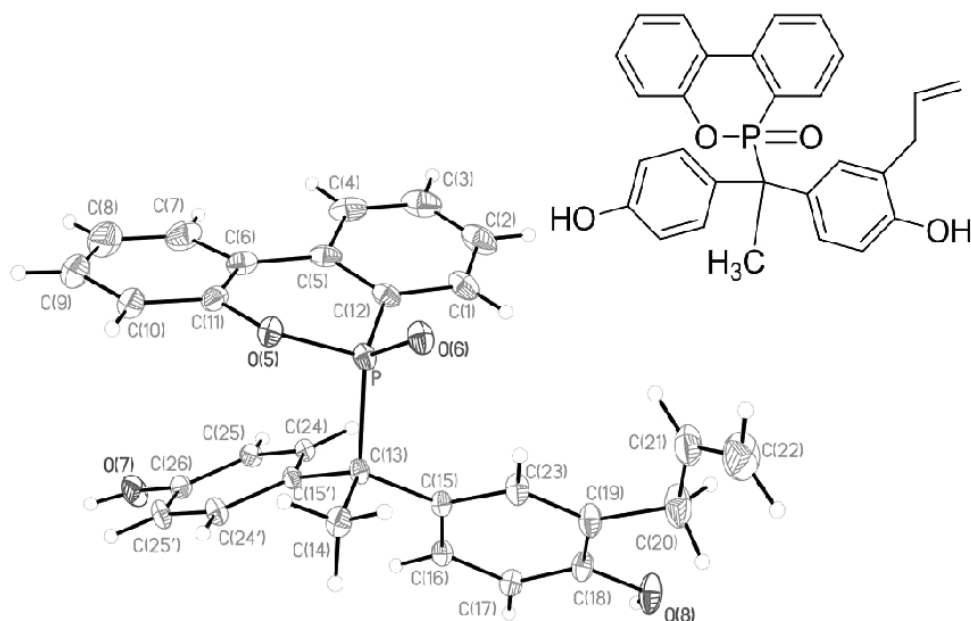


FIGURE 2 Single crystal diffractogram of (1).

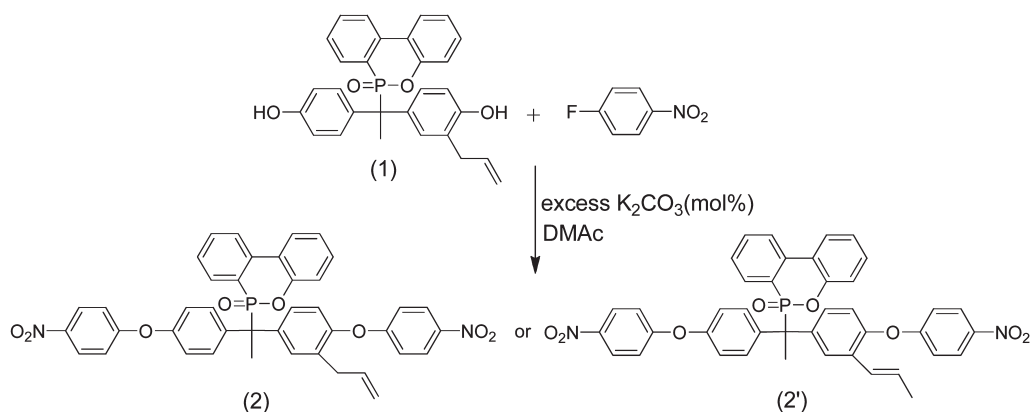
we believe that the nucleophilic substitution of (1) and 4-fluoronitrobenzene in the presence of excess potassium carbonate might lead to two products, (2) and (2') (Scheme 2).

Figure 3 shows the $^1\text{H-NMR}$ spectra of the reaction product prepared with several potassium carbonate-to-(1) ratios at $110\text{ }^\circ\text{C}$ for 12 h. Small propenyl peaks at 1.8, 5.9, and 6.2 ppm were found when the ratio of potassium carbonate-to-(1) was higher than 1.0 (Note that we found that the isomerization of the allyl chains to propenyl is strongly dependent on the reactant. Obvious isomerization was found in other systems, and the result will be published elsewhere.). For the molar ratio of ≤ 1 , [Figs. 3(a,b)], no signals from the isomerization of the allyl chains to propenyl moieties were found. In addition, the allyl signals at 5.8 (H^{21}), 4.9 (H^{22}), and 3.1 (H^{20}) clearly remained, suggesting that (2) was successfully prepared under the reaction condition. Supporting Information Figure S4 shows the detailed $^1\text{H-NMR}$ spectrum of (2). Compared with the $^1\text{H-NMR}$

spectrum of (1) (Fig. 1), the signals from $\text{H}^{28}\text{--H}^{28'}$ and $\text{H}^{29}\text{--H}^{29'}$ indicate that (2) was successfully prepared. Owing to the inductive and anisotropic deshielding effect of the nitro group, the signals of H^{29} and $\text{H}^{29'}$ (ortho to nitro group) show the highest chemical shift at around 8.3 ppm. In contrast, the signals of H^{17} , H^{25} , H^{28} , and $\text{H}^{28'}$ (ortho to ether group) show low chemical shift at 6.9–7.1 ppm because of the shielding effect of the electron-donating ether group. Other spectroscopic data such as $^{13}\text{C-NMR}$, $^1\text{H}\text{--}^1\text{H}$ COSY, and $^1\text{H}\text{--}^{13}\text{C}$ HETCOR spectra are shown in Supporting Information Figures S5–S7.

Synthesis of (3)

Initially, we reduced (2) via the hydrogen catalytic reduction in the presence of Pd/C. An amino peak at 5.0 ppm was clearly observed (Supporting Information Fig. S8). However, the signals from the allyl group disappeared completely, and new signals for propyl linkage at 0.8 (CH_3), 1.4 (CH_2), and 2.4 ($\text{Ph}\text{--CH}_2$) ppm appeared. This indicates that the reduction occurred not only on the nitro groups, but also on the



SCHEME 2 Synthesis of (2) and (2').

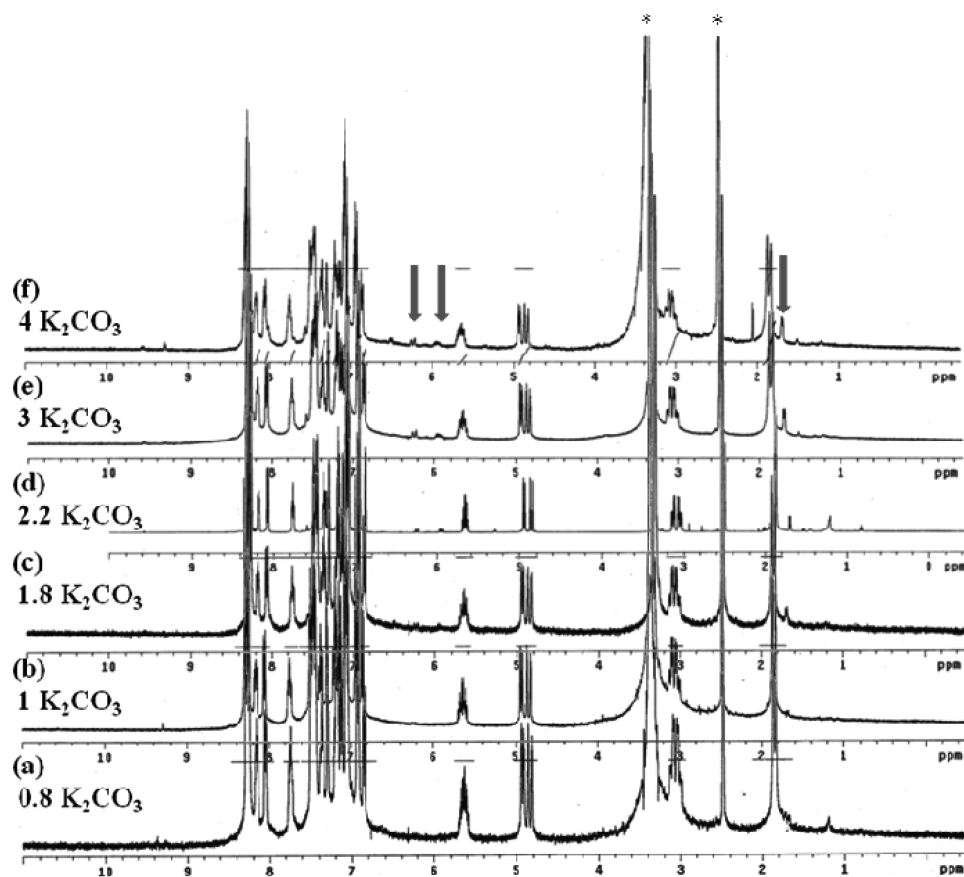


FIGURE 3 ^1H -NMR spectra of the reaction product prepared with several potassium carbonate-to-(1) ratios at 110°C for 12 h.

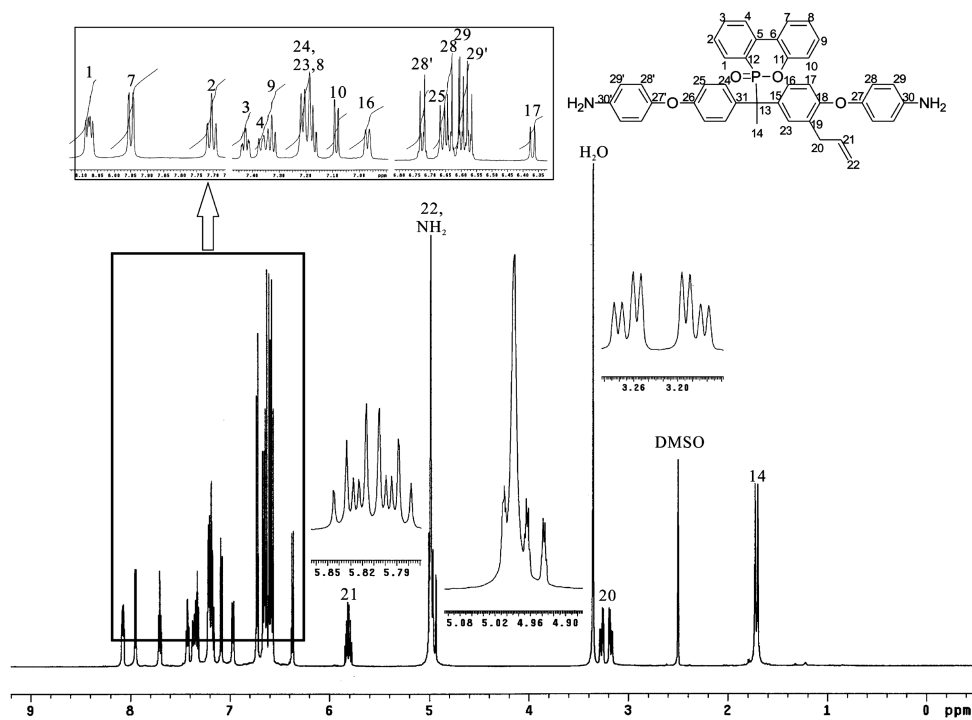
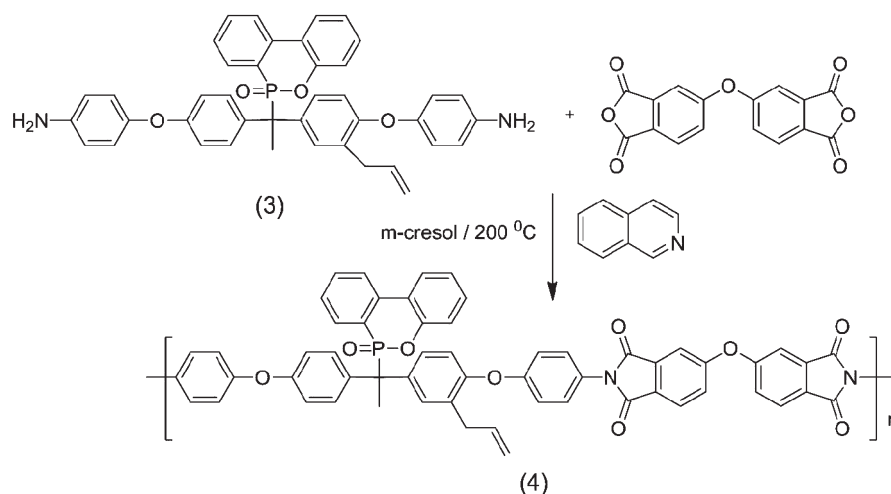


FIGURE 4 ^1H NMR spectrum of (3) in $\text{DMSO}-d_6$.



SCHEME 3 Synthesis of PEI (4).

allyl group. We then used Fe/HCl as the reduction agent.⁴² We found that the nitro was successfully reduced to amine, whereas the allyl group was preserved (Fig. 4). Because of the shielding effect of the electron-donating amino groups, signals of H²⁹ and H^{29'} upshifted from 8.3 ppm in (2) to 6.6 ppm in (3), demonstrating the successful reduction of (2). The other spectroscopic data, such as ¹³C-NMR, ¹H–¹H COSY, and ¹H–¹³C HETCOR spectra (Supporting Information Figs. S9–S11), support the structure and purity of (3).

PEI Synthesis

PEI (4) was prepared by the solution polymerization of (3) with ODPA in *m*-cresol in the presence of isoquinoline (Scheme 3). Supporting Information Figure S12 shows the ¹H-NMR spectrum of (4). Signals for the allyl group were clearly observed, suggesting that the allyl group is stable at this stage.

Supporting Information Figure S13 shows the DSC thermogram of (1). The allyl group, although relatively stable for free radical polymerization in mild conditions, can undergo

polymerization at high temperature, as supported by the exothermic peaks at around 252 and 280 °C. Therefore, a thermal curing of (4) at 300 °C resulted in a thermosetting (5). Figure 5 shows the enlarged IR spectra of (4) and (5). The intensity of allyl absorption at 920 cm⁻¹ clearly decreased,⁴⁰ supporting the curing characteristic of the allyl group at high temperatures.

Film Quality and Thermal Properties

Supporting Information Figure S14 shows a image of (4) and (5), in which both PEIs are flexible. As both films are flexible, DMA and TMA were applied to evaluate their thermal mechanical properties and dimensional stability. Figure 6 shows the DMA thermograms of (4) and (5). The *T*_g obtained from the peak temperature of tan(δ) increased from 253 °C for (4) to 307 °C for (5). An increase in modulus after glass transition was observed for (4). The increase is thought to be related to the increased rigidity of (4) owing to the curing of the allyl groups. The increased rigidity can also be supported by the smaller tan(δ) height of (5) compared to that of (4). Figure 7 shows the TMA curves of

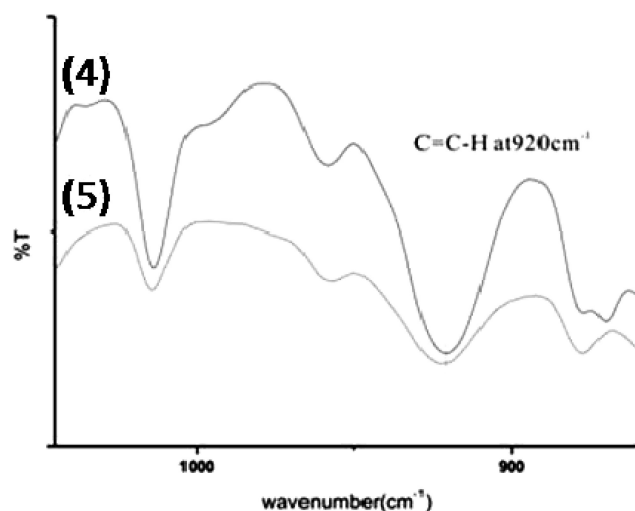


FIGURE 5 IR spectra of PEIs (4) and (5).

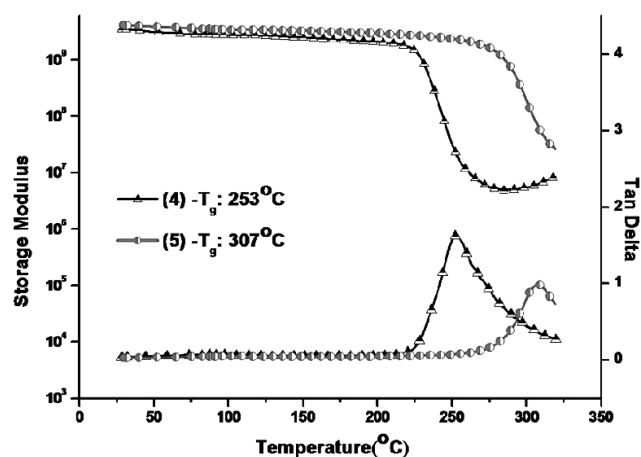


FIGURE 6 DMA thermograms of (4) and (5).

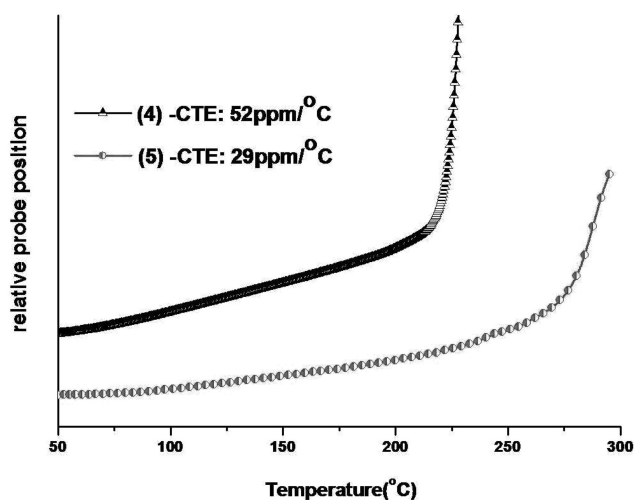


FIGURE 7 TMA thermograms of (4) and (5).

(4) and (5). The T_g obtained from the onset of dimension transition increased from 225 °C for (4) to 277 °C for (5). Both figures demonstrate the advantage of crosslinking in enhancing the T_g . Figure 7 also shows that the coefficient of thermal expansion (CTE) in the range of 50–150 °C decreased dramatically from 52 ppm/°C for (4) to 29 ppm/°C for (5). The CTE value is a relatively low one compared with other polyimides. This result points out the advantage of crosslinking in enhancing dimensional stability.

The thermal stability of both PEIs was evaluated by TGA (Supporting Information Figs. S15 and S16 and Table 1). The 5 wt % degradation temperature is 443 °C for (4), and 447 °C for (5) in a nitrogen atmosphere, and is 440 °C for (4) and 443 °C for (5) in an air atmosphere. The char yield is 54 wt % for (4) and 60 wt % for (5) in a nitrogen atmosphere, and 20 wt % for (4) and 41 wt % for (5) in an air atmosphere. Although significant enhancement in T_g and CTE was observed after thermal curing, the difference in the initial decomposition temperature for (4) and (5) is not as obvious in the case of the TGA thermograms. This result is reasonable as P–C is the weakest bond in both systems. Therefore, the effect of crosslinking is not obvious in the initial thermal decomposition. However, the effect of crosslinking in enhancing char yield is obvious.

TABLE 1 Thermal Properties of (4) and (5)

Sample	Film Quality	T_g (°C) (DMA) ^a	T_g (°C) (TMA) ^b	CTE (ppm/°C) ^c	$T_{d5\%}$ (°C) ^d		Char Yield ^e (wt %)	
					In N ₂	In air	In N ₂	In air
(4)	Flexible	253	225	52	443	440	54	20
(5)	Flexible	307	277	29	447	443	60	41

^a The peak temperature of $\tan \delta$, measured by DMA at a heating 5 °C/min.

^b Measured by TMA at a heating rate of 5 °C/min.

^c Coefficient of thermal expansion in the range of 50–150 °C.

^d Temperature corresponding to 5% weight loss, as recorded by TGA at a heating rate of 20 °C/min.

^e Residual weight percent at 800 °C.

TABLE 2 Data of UL-94 VTM Test for (4), (5), and Kapton

Sample Code	First Burning Time (s)	Second Burning Time (s)	Dripping	UL-94 Grade
(4)	1.6	0.4	No	V-0
(5)	1.2	0.3	No	V-0
Kapton	4.6	1.8	No	V-0

The flame retardancy of both systems was measured by a UL-94VTM vertical thin test (Table 2). The $t_1 + t_2$ took <3 s for both systems. Therefore, they belong to the VTM-0 grade. In contrast, the $t_1 + t_2$ took more than 6 s for Kapton. Although Kapton also belongs to the VTM-0 grade, the shorter total burning time of (4) and (5) demonstrates the excellent flame retardancy provided by the phosphorus element.

CONCLUSIONS

We have successfully prepared an allyl-containing diphenol (1) based on the reaction of DOPO, 4-hydroxyacetophenone, and 2-allylphenol in the presence of p-TSA. A dietheramine (3) with an allyl group was prepared from a potassium carbonate-catalyzed nucleophilic aromatic substitution of (1) with 4-fluoronitrobenzene, followed by the reduction of the dinitro compound (2). We found that the molar ratio of potassium carbonate-to-(1) influenced the purity of (2). No isomerization of the allyl chains to propenyl moiety was found when the ratio was ≤ 1 . We also found that Fe/HCl is a better reducing agent than the Pd/C, H₂ system, which leads to the reduction of the allyl bond simultaneously. PEI (4) prepared from (3) and OPDA in *m*-cresol shows a curable characteristic, as supported by the reduction of the IR absorption of the allyl group at 920 cm⁻¹ after thermal treatment. After curing (4) at 300 °C for 1 h, T_g shifted from 253 to 307 °C, and CTE decreased from 52 to 29 ppm/°C. This study provides an approach for transferring soluble PEIs to high T_g , high dimensional stability thermosetting PEIs.

ACKNOWLEDGMENT

The authors thank the National Science Council of the Republic of China for financial support.

REFERENCES AND NOTES

- 1 D.-J. Liaw, K.-L. Wang, Y.-C. Huang, K.-R. Lee, J.-Y. Lai, C.-S. Ha, *Prog. Polym. Sci.* **2012**, *37*, 907–974.
- 2 C.-L. Chung, C.-P. Yang, S.-H. Hsiao, *J. Polym. Sci. Part A: Polym. Chem.* **2006**, *44*, 3092–3102.
- 3 H.-S. Li, J.-G. Liu, J.-M. Rui, L. Fan, S.-Y. Yang, *J. Polym. Sci. Part A: Polym. Chem.* **2006**, *44*, 2665–2674.
- 4 S. M. Kwak, J. H. Yeon, T. H. Yoon, *J. Polym. Sci. Part A: Polym. Chem.* **2006**, *44*, 2567–2578.
- 5 T. Ogura, T. Higashihara, M. Ueda, *J. Polym. Sci. Part A: Polym. Chem.* **2010**, *48*, 1317–1323.
- 6 G.-S. Liou, P.-H. Lin, H.-J. Yen, Y.-Y. Yu, W.-C. Chen, *J. Polym. Sci. Part A: Polym. Chem.* **2010**, *48*, 1433–1440.
- 7 C.-Y. Wang, G. Li, J.-M. Jiang, *Polymer* **2009**, *50*, 1709–1716.
- 8 L. Tao, H. Yang, J. Liu, L. Fan, S. Yang, *Polymer* **2009**, *50*, 6009–6018.
- 9 T. Kurose, V. E. Yudin, J. U. Otaigbe, V. M. Svetlichnyi, *Polymer* **2007**, *48*, 7130–7138.
- 10 C. P. Yang, W. T. Chen, *Macromolecules* **1993**, *26*, 4865–4871.
- 11 C.-P. Yang, W.-T. Chen, *J. Polym. Sci. Part A: Polym. Chem.* **1993**, *31*, 1571–1578.
- 12 J. Hao, M. Jikei, M. A. Kakimoto, *Macromolecules* **2003**, *36*, 3519–3528.
- 13 I. S. Chung, S. Y. Kim, *Macromolecules* **2000**, *33*, 3190–3193.
- 14 H. Choi, I. S. Chung, K. Hong, C. E. Park, S. Y. Kim, *Polymer* **2008**, *49*, 2644–2649.
- 15 Y.-T. Chern, J.-Y. Tsai, J.-J. Wang, *J. Polym. Sci. Part A: Polym. Chem.* **2009**, *47*, 2443–2452.
- 16 W. G. Kim, A. S. Hay, *Macromolecules* **1993**, *26*, 5275–5280.
- 17 Y.-T. Chern, M.-H. Ju, *Macromolecules* **2008**, *42*, 169–179.
- 18 Y.-T. Chern, J.-Y. Tsai, *Macromolecules* **2008**, *41*, 9556–9564.
- 19 S.-H. Hsiao, K.-H. Lin, *J. Polym. Sci. Part A: Polym. Chem.* **2005**, *43*, 331–341.
- 20 Y. Liu, Y. Xing, Y. Zhang, S. Guan, H. Zhang, Y. Wang, Y. Wang, Z. Jiang, *J. Polym. Sci. Part A: Polym. Chem.* **2010**, *48*, 3281–3289.
- 21 Y.-C. Kung, G.-S. Liou, S.-H. Hsiao, *J. Polym. Sci. Part A: Polym. Chem.* **2009**, *47*, 1740–1755.
- 22 A. S. Mathews, D. Kim, Y. Kim, I. Kim, C.-S. Ha, *J. Polym. Sci. Part A: Polym. Chem.* **2008**, *46*, 8117–8130.
- 23 S. Wu, T. Hayakawa, M. A. Kakimoto, H. Oikawa, *Macromolecules* **2008**, *41*, 3481–3487.
- 24 Y. Zhuang, X. Liu, Y. Gu, *Polym. Chem.* **2012**, *3*, 1517–1525.
- 25 P. R. Buch, A. V. R. Reddy, *Polymer* **2005**, *46*, 5524–5532.
- 26 G. Maglió, R. Palumbo, A. Schioppa, D. Tesauro, *Polymer* **1997**, *38*, 5849–5856.
- 27 C. Lee, N. P. Iyer, K. Min, H. Pak, H. Han, *J. Polym. Sci. Part A: Polym. Chem.* **2004**, *42*, 137–143.
- 28 H. Behniafar, S. Habibian, *Polym. Int.* **2005**, *54*, 1134–1140.
- 29 T. Iijima, N. Hayashi, T. Oyama, M. Tomoi, *Polym. Int.* **2004**, *53*, 1417–1425.
- 30 G. W. Meyer, J. L. Heidbrink, J. G. Franchina, R. M. Davis, S. Gardner, V. Vasudevan, T. E. Glass, J. E. McGrath, *Polymer* **1996**, *37*, 5077–5088.
- 31 T. Kuroki, A. Shibuya, M. Toriida, S. Tamai, *J. Polym. Sci. Part A: Polym. Chem.* **2004**, *42*, 2395–2404.
- 32 T. Sasaki, H. Moriuchi, S. Yano, R. Yokota, *Polymer* **2005**, *46*, 6968–6975.
- 33 J. A. Mikroyannidis, *J. Polym. Sci. Part A: Polym. Chem.* **1994**, *32*, 2403–2411.
- 34 A. J. Hu, J. Y. Hao, T. He, S. Y. Yang, *Macromolecules* **1999**, *32*, 8046–8051.
- 35 T. Pascal, D. Audigier, R. Mercier, B. Sillion, *Polymer* **1991**, *32*, 1119–1125.
- 36 L. Bes, A. Rousseau, B. Boutevin, R. Mercier, *J. Polym. Sci. Part A: Polym. Chem.* **2001**, *39*, 2602–2619.
- 37 L.-S. Tan, F. E. Arnold, *J. Polym. Sci. Part A: Polym. Chem.* **1988**, *26*, 1819–1834.
- 38 K. Xu, J. Economy, *Macromolecules* **2004**, *37*, 4146–4155.
- 39 N. Furukawa, M. Yuasa, Y. Yamada, Y. Kimura, *Polymer* **1998**, *39*, 2941–2949.
- 40 T. Fukuhara, Y. Shibasaki, S. Ando, M. Ueda, *Polymer* **2004**, *45*, 843–847.
- 41 J. M. Barton, A. Chaplin, I. Hamerton, B. J. Howlin, *Polymer* **1999**, *40*, 5421–5427.
- 42 K. Xie, S. Y. Zhang, J. G. Liu, M. H. He, S. Y. Yang, *J. Polym. Sci. Part A: Polym. Chem.* **2001**, *39*, 2581–2590.